Thermodynamic, Counterion, and Hydration Effects for the Incorporation of Locked Nucleic Acid Nucleotides into DNA Duplexes†

Harleen Kaur,‡ Amit Arora,‡ Jesper Wengel,§ and Souvik Maiti*,‡

Institute of Genomics and Integrative Biology, CSIR, Mall Road, Delhi 110 007, India, and Nucleic Acid Center, Department of Chemistry, University of Southern Denmark, DK-5230 Odense M, Denmark

Received February 14, 2006; Revised Manuscript Received April 7, 2006

ABSTRACT: A locked nucleic acid (LNA) monomer is a conformationally restricted nucleotide analogue with an extra 2′-*O*, 4′-*C*-methylene bridge added to the ribose ring. LNA-modified oligonucleotides are known to exhibit enhanced hybridization affinity toward complementary DNA and RNA. In this work, we have evaluated the hybridization thermodynamics of a series of LNA-substituted DNA octamers, modified to various extents by one to three LNA substitutions, introduced at either adenine (5′-AGCACCAG) or thymine (5′-TGCTCCTG) nucleotides. To understand the energetics, counterion effects, and the hydration contribution of the incorporation of LNA modification, a combination of spectroscopic and calorimetric techniques was used. The CD spectra of the corresponding duplexes showed that the modified duplexes adopt an A-type conformation. UV and DSC melting studies revealed that each type of duplex unfolds in a two-state transition. A complete thermodynamic profile at 5 °C indicated that the net effect of modification on thermodynamic parameters might be positional and that the neighboring bases flanking the modification might influence the favorable formation of the modified duplexes. Furthermore, relative to the formation of the unmodified reference duplexes, the formation of modified duplexes is accompanied by a higher uptake of counterions and a lower uptake of water molecules.

Nucleic acid recognition between two complementary nucleic acid strands by Watson−Crick hybridization is fundamental for a vast number of processes in molecular biology and is a complex interaction governed by subtle enthalpic and entropic contributions. During the past few decades, exploration and examination of nucleic acid hybridization has boomed, and efforts to exploit the immense potential of oligonucleotides as therapeutic tools in antisense and antigene strategies have been ongoing (*1*, *2*). In theory, the concept of executing oligonucleotide-based antisense and antigene strategies seems quite feasible, where high-affinity hybridization between the oligonucleotide and the target strand serves to alter or inhibit gene expression. But, in practice, the use of these strategies has fallen from favor because of the difficulties faced in predicting (i) the accessible sites or structures of the target against which the oligonucleotide has to be directed, (ii) the optimum dose levels required by the agent to act without mediating any toxic effects, and (iii) the inherent weaknesses associated with the oligonucleotide, particularly, specificity and biostability issues (*1*, *2*). The factors listed above have acted as triggers to uplift the development of novel, structurally modified oligonucleotides that could act as potent and more selective therapeutic agents.

Scheme 1 [a]

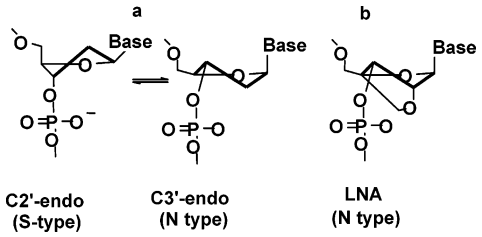

[a] (a) The C2′-endo−C3′-endo sugar ring equilibrium present in nucleic acids. (b) The molecular structure of locked nucleic acid (LNA), which shows the locked C3′-endo sugar conformation.

One of the most promising candidates of chemically modified nucleotides developed in the past few years is the locked nucleic acid (LNA) (Scheme 1). LNA nucleosides are ribonucleotide analogues containing a methylene linkage between 2′-O and 4′-C of the ribose ring. This constraint on the sugar moiety results in a locked 3′-endo conformation that preorganizes the LNA nucleotide monomers for high-affinity hybridization (*3*, *4*). Its close structural resemblance to DNA, exceptionally high affinity for the target strand, high specificity, high in vivo stability, lack of toxicity, and ease of transfection into cells have all contributed to its success as a promising tool for therapeutics and functional genomics (*5*−*8*). Furthermore, LNA oligonucleotides can be synthesized using conventional phosphoramidite chemistry, allowing automated synthesis of both fully modified LNA and for LNA−DNA and LNA−RNA chimeric oligonucleotides (*5*, *6*). Finally, the presence of the charged phosphate backbone allows their efficient delivery into the cells using

† S.M. acknowledges CSIR for funding (OLP 0047) this research. J.W. thanks The Danish National Research Foundation for funding The Nucleic Acid Center. A.A. acknowledges a research fellowship from CSIR.

* To whom correspondence should be addressed. Phone: +91-11-2766-6156. Fax: +91-11-2766-7471. E-mail: souvik@igib.res.in.

‡ CSIR.

§ University of Southern Denmark.

10.1021/bi060307w CCC: $33.50
Published on Web 05/17/2006

standard protocols employing cationic transfection agents (*6*, *7*).

The use of LNA as a therapeutic agent has made a revolutionary contribution to basic science and medicine. Several reports involving the successful employment of LNA technology to modulate gene expression are available, at the level of either DNA (*9*−*12*) or RNA (*13*−*24*). In addition to creating avenues for gene-based therapy, LNAs find wide application in diagnostics as probe molecules in hybridization-based assays such as SNP genotyping (*25*−*29*). The immense potential of LNA can be exploited in a number of ways and in combination with a number of other technologies. LNA is, thus, likely to make a strong impact on every sphere of biotechnology and medicine. However, the existing biophysical knowledge of hybridization thermodynamics of LNA, other than ΔT_m measurements, is limited. A few reports based on thermodynamic evaluation of LNA-mediated nucleic acid hybridization showed that the introduction of an LNA modification induces entropically favored duplex formation, compared to the unmodified duplexes, whereas duplex formation for the all-modified LNA appeared to be entropically disfavored and strongly enthalpically favored (*30*). Another study revealed a large positive $\Delta\Delta S$ and a negligible $\Delta\Delta H$ for a gapmer with seven LNAs (*8*). A hybridization kinetics study using stopped-flow kinetics has also been performed. Evaluation of thermodynamics for the same oligonucleotides showed small negative $\Delta\Delta H$ and $\Delta\Delta S$ values for LNA-modified duplex formation (*31*). Another study examined the sequence-dependent effects of LNA substitutions on thermodynamic parameters (*32*). The studies mentioned above represent a preliminary evaluation of LNA-mediated hybridization thermodynamics, based on simple UV melting experiments. What is more required is the detailed insight into the biophysical and molecular aspects of hybridization thermodynamics and kinetics of LNAs. This will not only facilitate the optimum designing of LNA based oligonucleotides but also allow researchers to predict and design the architecture of more advanced analogues with superior properties and higher efficiency.

With this aim, we have made an attempt to characterize the hybridization thermodynamics of LNA-substituted oligonucleotides, to account for their high binding efficiency toward the complementary strand. For all the modified oligonucleotides, substitutions were introduced at adenine or thymine nucleotides. Complete thermodynamic profile for duplex formation at 5 °C suggests that the net effect of the LNA modification on thermodynamic parameters might be position-dependent or influenced by neighboring bases flanking the modification. We observed that for incorporation of the first (5′-XG-3′, where X is the modified LNA nucleotide) and third modification (5′-CXG-3′), stabilization of duplex formation results from a large and favorable increase in the enthalpy of hybridization that compensates for the unfavorable entropy change. However, incorporation of the second modification (5′-CXC-3′) is associated with a favorable entropy change that compensates for an unfavorable enthalpy change. Further, the formation of the LNA-modified duplex is associated with the higher uptake of sodium ions and lower uptake of water molecules with respect to the unmodified duplex.

Table 1: Duplexes Used with LNA Modifications with an L Superscript

nomenclature	sequence (8-mer)
T-LNA0	5′-TGCTCCTG-3′ 3′-ACGAGGAC-5′
T-LNA1	5′-T^{L}GCTCCTG-3′ 3′-ACGAGGAC-5′
T-LNA2	5′-T^{L}GCT^{L}CCTG-3′ 3′-ACGAGGAC-5′
T-LNA3	5′-T^{L}GCT^{L}CCT^{L}G-3′ 3′-ACGAGGAC-5′
A-LNA0	5′-AGCACCAG-3′ 3′-TCGTGGTC-5′
A-LNA1	5′-A^{L}GCACCAG-3′ 3′-TCGTGGTC-5′
A-LNA2	5′-A^{L}GCA^{L}CCAG-3′ 3′-TCGTGGTC-5′
A-LNA3	5′-A^{L}GCA^{L}CCA^{L}G-3′ 3′-TCGTGGTC-5′

EXPERIMENTAL PROCEDURES

To study the hybridization thermodynamics of LNA-based oligonucleotides, two sets of 8-mer oligonucleotides were considered. The oligonucleotides were modified to various extents and at various positions with either adenine- or thymine-locked nucleic acid nucleotides. For each of the A- and T-modified sets, four oligonucleotide sequences, containing LNA substitutions ranging from zero to three modified nucleotides, were studied (Table 1).

All the LNA-containing octamers were synthesized and purified as described in the literature (*5*). The other unmodified oligonucleotides (HPLC-purified) were purchased from Sigma Genosys. The solution concentrations of each of the unmodified oligonucleotide were determined optically at 260 nm and 25 °C using the following molar extinction coefficients (per mM^{-1} cm^{-1} of strands): 81.3 for d(AGCACCAG), 68.3 for d(CTGGTGCT), 65.7 for d(TGCTCCTG), and 84.1 for d(CAGGAGCA). These values were calculated by extrapolation of the tabulated values of the dimer and monomer nucleotides (*33*) at 25 °C to high temperatures using protocols reported previously (*34*). For the modified oligonucleotides, the molar absorptivities were assumed to be identical to the DNA oligonucleotides.

All the measurements were performed in 10 mM sodium cacodylate buffer (pH 7). The duplex solutions were prepared by mixing the given template strand, bearing varying amount of LNA modifications, with the corresponding unmodified complementary strand in a 1:1 ratio.

Circular Dichroism (CD) Spectroscopy. Evaluation of the conformation of each duplex (Table 1) was carried out by inspection of their CD spectra. The spectra were obtained on a Jasco circular dichroism spectrometer (model 715), using a 10 mm quartz cuvette. All spectra were collected at 10 °C between 200 and 350 nm, using a wavelength step of 1 nm. The reported spectra corresponded to the average of at least two scans.

Temperature-Dependent UV Spectroscopy (UV Melts). Absorbance versus temperature profiles (melting curves) for each duplex were measured at 260 nm with a thermoelectrically controlled Cary 400 (Varian) spectrophotometer, as a function of salt (10−110 mM Na^+) and osmolyte [5−25% (w/v) ethylene glycol] concentration. The temperature was scanned at a heating rate of 1 °C/min. The mole fraction of

the folded oligonucleotide (α) at different temperatures was evaluated from the absorbance, and $\Delta A/\Delta A_{max}$, where ΔA is the change in absorbance at 260 nm at any temperature and ΔA_{max} is the maximum change recorded at the highest temperature, was also calculated. The plot of mole fraction (α) or $\Delta A/\Delta A_{max}$ versus temperature allowed us to measure the melting temperature, T_m.

Differential Scanning Calorimetry (DSC Melts). To investigate the helix−coil transition of each duplex (10 μM), excess heat capacities as a function of temperature (melting curves) were measured with Microcal (Northampton, MA) MC-2 or VP-differential scanning calorimeters. Two cells, the sample cell containing 1.4 mL (MC-2 DSC) or 0.52 mL (VP DSC) of an oligonucleotide solution and the reference cell filled with the same volume of buffer solution, were heated from 10 to 90 °C at a heating rate of 1 °C/min. Analysis of the resulting thermograms using procedures described previously (*35*) yielded standard thermodynamic profiles (ΔH_{cal}, ΔS_{cal}, ΔC_p, and $\Delta G°_{cal}$) and model-dependent van't Hoff enthalpies (ΔH_{vH}) for the transition of each duplex.

Data Analysis. The van't Hoff enthalpy (ΔH_{vH}) change for the helix−coil transition was obtained from UV melting as described in the literature (*34*). The thermodynamic uptake of counterions, Δn_{Na^+}, associated with the process of duplex formation can be obtained according to the equation

$$\Delta n_{Na^+} = 1.11(\Delta H/RT_m^2)\, \delta T_m/\delta(\ln[Na^+]) \qquad (1)$$

where 1.11 is a proportionality constant for converting ionic activity into concentrations and $\delta T_m/\delta(\ln[Na^+])$ represents the slope of a plot of T_m versus the logarithm of sodium ions ($\ln[Na^+]$) at different concentrations (10−110 mM Na^+) (*36*). The term in parentheses is a constant obtained from the DSC experiment, and R represents the universal gas constant (1.986 cal mol^{-1} K^{-1}).

Similarly, the changes in the number of water molecules associated with the melting process, Δn_W, were obtained from the dependence of T_m on water activity (a_W) according to the equation

$$\Delta n_W = (-\Delta H/R)[\delta(T_m^{-1})/\delta(\ln a_W)] \qquad (2)$$

where ΔH is the enthalpy change determined from DSC experiments and R is the universal gas constant (*37*). The slope of the plot of reciprocal temperature (K^{-1}) of melting versus the logarithm of water activity ($\ln a_W$) at different concentrations (0, 5, 10, 15, 20, and 25%) of ethylene glycol gave the value of $\delta(T_m^{-1})/\delta(\ln a_W)$.

Analysis of the resulting thermograms from DSC, using procedures reported previously (*35*) and assuming a negligible heat capacity effect, yielded standard thermodynamic profiles (ΔH_{cal}, ΔS_{cal}, and $\Delta G°_{cal}$). ΔH_{cal} and ΔS_{cal} were measured from the DSC curves according to the equations $\Delta H_{cal} = \int \Delta C_p\, dT$ and $\Delta S_{cal} = \int \Delta C_p/T\, dT$, respectively. $\Delta G°_{cal}$ was calculated at 5 °C from the Gibbs relationship $\Delta G°_{cal} = \Delta H_{cal} - T\Delta S_{cal}$ (*38*, *39*). Further, the effects of LNA incorporation on the thermodynamic parameters can be represented as the difference in the ΔH and ΔS for hybridization between the LNA-containing duplex and the unmodified duplex ($\Delta\Delta H = \Delta H_{LNA+DNA:DNA} - \Delta H_{DNA:DNA}$ and $\Delta\Delta S = \Delta S_{LNA+DNA:DNA} - \Delta S_{DNA:DNA}$). Shape analysis of the experimental DSC curve gave the van't Hoff enthalpy change ΔH_{vH}. The $\Delta H_{vH}/\Delta H_{cal}$ ratio allowed us to inspect if duplex unfolding takes place in two-state transitions or through the formation of intermediates. A $\Delta H_{vH}/\Delta H_{cal}$ ratio equal to 1 indicates that the transition takes place in an all-or-none fashion.

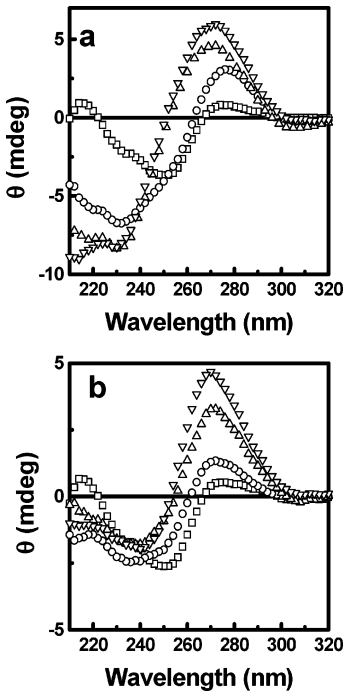

FIGURE 1: Circular dichroism spectra of the unmodified (□) and single (○), double (△), and triple (▽) modified duplexes (2.52 μM): (a) A-LNA and (b) T-LNA in 10 mM sodium cacodylate (pH 7.0), with 100 mM NaCl, at 10 °C.

RESULTS

Circular Dichroism Study. The CD spectra for all duplexes at 10 °C and at a duplex concentration of 2.52 μM are shown in Figure 1. As seen in the figure, the unmodified duplexes exhibited a positive peak at 275 nm and a negative peak at 250 nm, which is characteristic of a right-handed helix in a B-conformation. The CD spectra of the modified duplexes containing LNA bases were markedly different from those of the corresponding unmodified duplexes. For all the LNA-modified duplexes, a positive peak at 270 nm and a negative peak at 238 nm were observed, with a marked increase in the intensity, which was consistent with the increase in the extent of LNA modifications. The change in the signature of the modified duplex with respect to the unmodified duplex suggests that the presence of an LNA modification disrupts the B-conformation of the helix in the direction of A-type helix (*40*).

UV Melting Study. Oligonucleotides containing LNA substitutions are known to display enhanced thermal stability when hybridized to complementary DNA and RNA (*2*−*8*). As expected, the duplexes containing one, two, and three locked nucleotide monomers exhibited significantly higher T_m values than the corresponding unmodified DNA duplexes (Figure 2). The increment in T_m per modification for A-LNA was found to be 2.0 (A-LNA1), 1.5 (A-LNA2), and 2.7 °C (A-LNA3), whereas increase of 2.0 (T-LNA1), 2.0 (T-LNA2), and 3.0 °C (T-LNA3) were recorded for T-LNA

Table 2: Melting Temperatures (T_m Values) at Two Different Salt Concentrations and van't Hoff Enthalpy Changes for the Helix−Coil Transition

	T_m (°C)				
duplex	10 mM Na^+	increase per modification	110 mM Na^+	increase per modification	ΔH_{vH} (kcal/mol)[a]
A-LNA0	21.0	−	30.5	−	−60.2
A-LNA1	23.0	2	33.3	2.8	−69.7
A-LNA2	24.0	1.5	35.0	2.25	−59.9
A-LNA3	29.0	2.7	41.6	3.7	−62.2
T-LNA0	18.0	−	28.5	−	−54.3
T-LNA1	20.0	2	31.0	2.5	−64.4
T-LNA2	22.0	2	34.0	2.75	−60.0
T-LNA3	27.0	3	41.0	4.1	−57.0

[a] All the parameters were obtained from UV experiments. Duplex concentrations were 1.26 μM. Experiments were conducted in 10 mM sodium cacodylate buffer (pH 7.0). The ΔH_{vH} is obtained as described in the text. T_m values are within 0.5 °C. ΔH_{vH} values are averages of five values and within 10% error.

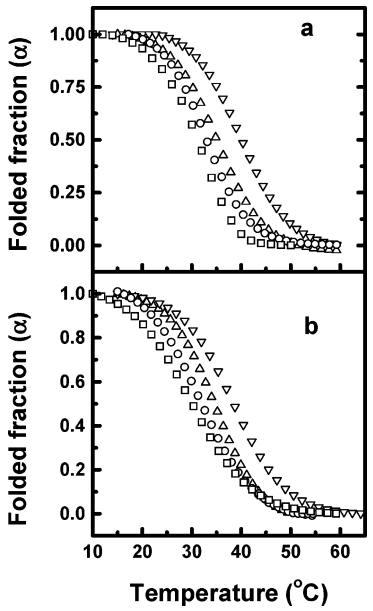

FIGURE 2: UV melting curves of unmodified (□) and single (○), double (△), and triple (▽) modified oligonucleotides in 10 mM sodium cacodylate buffer with 100 mM NaCl: (a) A-LNA and (b) T-LNA.

duplexes at 10 mM Na^+. A more prominent enhancement in T_m was obtained at a higher salt concentration of 110 mM Na^+, where a higher T_m increment per modification was detected for both the A-LNA and T-LNA duplexes (Table 2). In each case, the enhancement in the T_m value was higher for T-LNA modification than for A-LNA modification.

DSC Melting Study. The DSC melting curves for each of the duplexes are shown in Figure 3, and their complete thermodynamic profiles determined from these curves at 5 °C are summarized in Table 3. Table 3 also depicts the effects of LNA incorporation on the thermodynamic parameters. It was observed that for all the modified duplexes except A-LNA2 and T-LNA2, a negative $\Delta\Delta H$ (indicating a favorable enthalpy change) and a negative $\Delta\Delta S$ (indicating an unfavorable entropy loss) were obtained. For A-LNA2 and T-LNA2, the change in the thermodynamic parameters involved an unfavorable enthalpy change and a favorable entropy change. Table 3 also shows the van't Hoff enthalpies calculated from the shape analysis of DSC curves. The $\Delta H_{vH}/\Delta H_{cal}$ ratios of 1.08−1.13 obtained for the duplexes indicate that these molecules unfold in two-state transitions; that is, the transitions occur in an all-or-none fashion without the presence of any intermediate states (*35*).

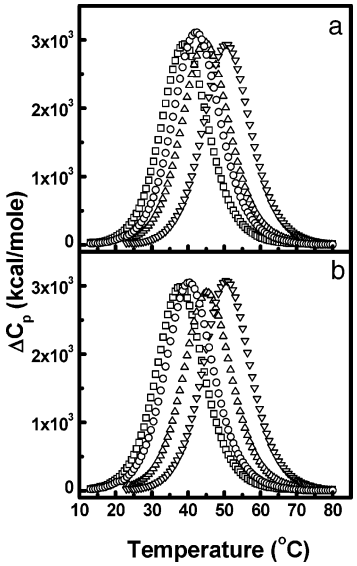

FIGURE 3: Typical DSC curves of duplex melting in 10 mM sodium cacodylate buffer (pH 7.0) with 100 mM NaCl for (a) A-LNA0 (□), A-LNA1 (○), A-LNA2 (△), and A-LNA3 (▽) and (b) T-LNA0 (□), T-LNA1 (○), T-LNA2 (△), and T-LNA3 (▽).

Counterion Uptake upon Duplex Formation. Sodium ions are known to bind to DNA in various forms. These condensed ions contribute to the stability of helical structures by reducing the repulsive forces between phosphate groups along the chain (*41*). When the DNA duplex melts, there is release of Na^+ ions due to the reduction of charge density along the chain in conversion of helical duplex DNA to single strands (*42*). To estimate the effect of LNA modification on the counterion uptake associated with the process of duplex formation, UV melting curves of duplexes (1.26 μM) at several salt concentrations (10−110 mM Na^+) were studied. A representative curve for A-LNA3 and T-LNA3 is shown in Figure 4. The increase in the salt concentration resulted in the shift of curves to higher temperatures. This is the characteristic effect of salt, stabilizing the duplex state with a higher negative charge density parameter. The dependence of T_m on salt concentration is shown in Figure 5 for each duplex. The slopes of these lines are listed in Table 4. The counterion uptake for each duplex (Table 4) over this range of salt concentration was calculated using eq 1. It was observed that introduction of the modification into one of the oligonucleotide strands of the duplex leads to a higher uptake of counterions (sodium ions) upon duplex formation.

Uptake of Water Molecules upon Duplex Formation. Any equilibrium that involves changes in the water molecules associated with a biopolymer is sensitive to changes in the water activity (a_W) (*43, 44*). Water activity can in turn be manipulated by the addition of low-molecular weight cosolutes, which themselves do not interact with the biopolymer but are assumed to change the water activity. A straightforward equation can then be applied, which gives the number of water molecules uniquely bound to the double helix and that are released upon melting or unfolding of the duplex (*37*). To detect the differences in the hydration of duplexes

Table 3: Thermodynamic Profiles for the Formation of Duplexes at 5 °C[a]

duplex	T_m (°C)	ΔH_{cal} (kcal/mol)	ΔH_{vH} (kcal/mol)	$\Delta H_{cal}/\Delta H_{vH}$	ΔS (eu)	$\Delta G°$(5 °C) (kcal/mol)	$\Delta\Delta H$ (kcal/mol)	$\Delta\Delta S$ (eu)	$\Delta\Delta G°$ (kcal/mol)
A-LNA0	38.1	−57.3	−59.8	1.04	−184	−6.10			
A-LNA1	41.8	−59.1	−64.1	1.08	−188	−6.91	−1.80	−4	−0.81
A-LNA2	44.8	−57.1	−60.0	1.04	−181	−7.15	0.20	4	−0.24
A-LNA3	50.6	−60.0	−65.5	1.09	−185	−8.45	−2.70	−1	−1.30
T-LNA0	37.3	−58.4	−61.5	1.05	−188	−6.08			
T-LNA1	40.3	−60.1	−66.1	1.10	−192	−6.77	−1.70	−4	−0.69
T-LNA2	44.7	−57.9	−61.5	1.06	−182	−7.24	0.50	6	−0.46
T-LNA3	50.7	−63.0	−66.0	1.05	−195	−8.89	−4.60	−7	−1.65

[a] All the parameters were obtained from DSC experiments. Duplex concentrations were 10 μM. Experiments were conducted in 10 mM sodium cacodylate buffer (pH 7.0) with 100 mM Na^+. ΔH_{vH} values were obtained from the shape of calorimetric curves. T_m values are within 0.5 °C. ΔH_{cal} values are within 3% error. $\Delta G°$ and ΔS values are within 5% error. ΔH_{vH} values are within 10% error.

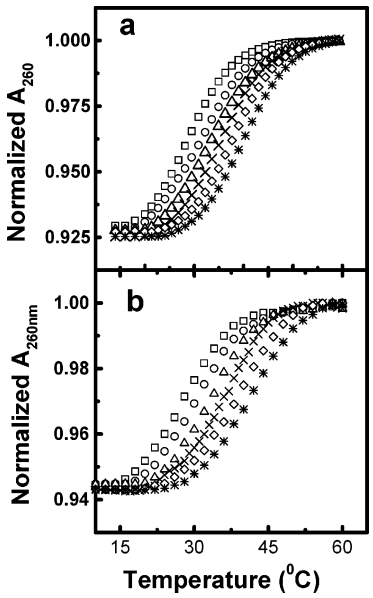

FIGURE 4: Typical UV melting curves of (a) A-LNA3 and (b) T-LNA3 over a Na^+ concentration range of 10−110 mM, in 10 mM sodium cacodylate (pH 7.0), and at a constant strand concentration of 1.26 μM. Curves correspond to sodium concentrations of 10 (□), 20 (○), 30 (△), 40 (×), 60 (◇), and 110 mM (∗).

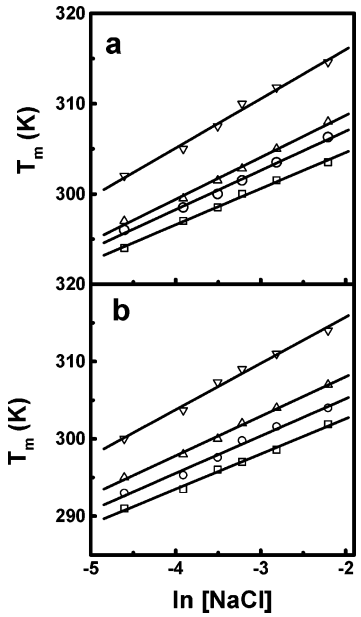

FIGURE 5: T_m dependence on salt concentration shown for (a) A-LNA0 (□), A-LNA1 (○), A-LNA2 (△), and A-LNA3 (▽) and for (b) T-LNA0 (□), T-LNA1 (○), T-LNA2 (△), and T-LNA3 (▽).

induced by the incorporation of LNA nucleotide modifications, ethylene glycol was used as the cosolute.

UV melting curves of each duplex (2.52 μM) at several concentrations of ethylene glycol (0−25%) and at 100 mM NaCl were obtained. A representative curve for A-LNA3 and T- LNA3 is shown in Figure 6. In each case, the increase in the osmolyte concentration shifts the T_m of melting curves to lower temperatures. The $1/T_m$ dependence on ln a_W is shown in Figure 7 for each duplex. The rate of thermodynamic uptake of water molecules upon formation of the duplex was calculated using eq 2. The slope of these plots, along with the corresponding change in the number of water molecules taken up by the duplexes, is given in Table 4. It was observed that increasing the number of LNA nucleotides led to a lower uptake of water molecules by the modified duplexes as compared to the unmodified duplex, suggesting that the modified duplexes are less hydrated than their corresponding unmodified counterparts.

DISCUSSION

A locked nucleic acid (LNA) is an RNA mimic with a conformationally constrained sugar moiety, which displays unprecedented hybridization affinity toward complementary DNA and RNA with high sequence specificity. This feature of LNA along with a number of other desirable properties has established it as a promising molecule for the development of oligonucleotide-based therapeutics. A remarkable freedom exists for the design of high-affinity LNAs, both as fully modified LNA and as LNA−DNA or LNA−RNA chimera, also combined with other modifications such as phosphorothioate linkages or 2′-*O*-Me-RNA. This flexibility in design allows wide applications of LNA in a diverse number of fields and in combination with a number of different technologies. However, optimum designing requires a thorough understanding of the hybridization thermodynamics and kinetics of LNA-modified duplexes. A complete insight into the above-mentioned aspect will aid in predicting the choice of model, for a given application such that maximum efficiency can be drawn out of a minimum modification. In this study, for the first time we have characterized the thermodynamics, counterions, and hydration changes associated with the incorporation of LNA nucleotides in one of the strands of the duplex.

Structural perturbations produced by incorporation of LNA modifications have been addressed in few reports (*45*, *46*) where CD spectra and NMR experiments for LNA-modified duplexes revealed resemblance to the A-form duplex. Our

Table 4: Thermodynamic Uptake of Counterions and Water Molecules upon Duplex Formation[a]

duplex	$\delta(T_m)/\delta[Na^+]$ (°C)	Δn_{Na^+} (per duplex)	$\delta(1/T_m)/\delta(\ln a_W)$ ($°C^{-1}$)	Δn_w (per duplex)	$\Delta\Delta n_{Na^+}$	$\Delta\Delta n_w$
A-LNA0	4.00	−2.63	-5.32×10^{-4}	−15.4		
A-LNA1	4.35	−2.88	-4.08×10^{-4}	−12.1	−0.25	3.30
A-LNA2	4.65	−2.91	-3.89×10^{-4}	−11.2	−0.28	4.20
A-LNA3	5.56	−3.53	-3.03×10^{-4}	−9.2	−0.90	6.38
T-LNA0	4.54	−3.05	-5.04×10^{-4}	−14.8		
T-LNA1	4.81	−3.27	-4.66×10^{-4}	−14.1	−0.22	0.70
T-LNA2	5.10	−3.25	-3.09×10^{-4}	−9.0	−0.20	5.80
T-LNA3	5.99	−3.99	-2.21×10^{-4}	−7.0	−0.94	7.80

[a] Experiments were conducted in 10 mM sodium cacodylate buffer, at pH 7.0, and concentrations of sodium chloride or ethylene glycol were adjusted. Experiments with ethylene glycol were conducted in 10 mM sodium cacodylate buffer containing 100 mM Na^+. $\delta(T_m)/\delta[Na^+]$ and $\delta(1/T_m)/\delta(\ln a_W)$ values are within 5%, and Δn_{Na^+} and Δn_W values are within 10% error. Duplex concentrations were 1.26 and 2.52 μM for salt- and osmolyte-dependent studies, respectively.

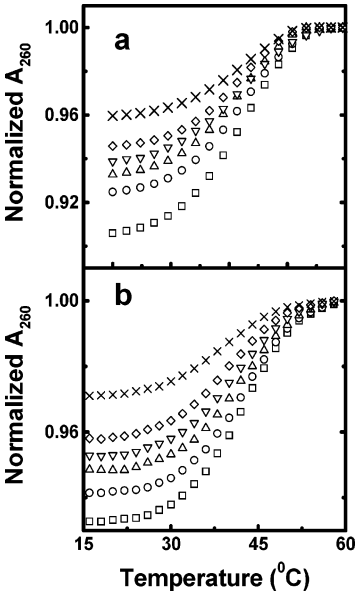

FIGURE 6: Typical UV melting curves at a constant strand concentration of 2.52 μM, as a function of ethylene glycol concentration in 10 mM sodium cacodylate buffer (pH 7.0), with 100 mM Na^+: (a) A-LNA3 and (b) T-LNA3. Curves correspond to ethylene glycol concentrations of 0 (□), 5 (○), 10 (△), 15 (▽), 20 (◇), and 25% (×) (w/v).

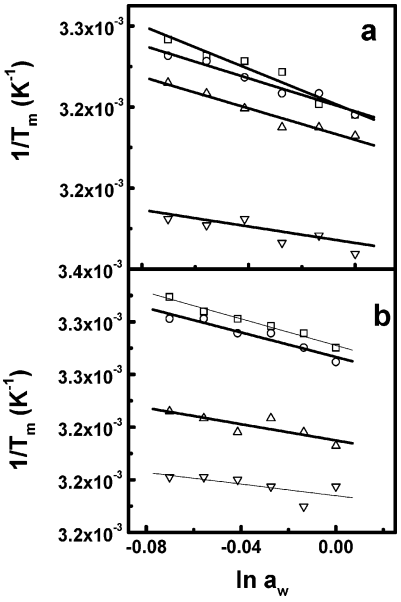

FIGURE 7: Dependence of $1/T_m$ on ln a_w: (a) A-LNA0 (□), A-LNA1 (○), A-LNA2 (△), and A-LNA3 (▽) and (b) T-LNA0 (□), T-LNA1 (○), T-LNA2 (△), and T-LNA3 (▽).

CD data (Figure 2) supported this finding where we observed the inherent tendency of DNA−LNA duplexes to adopt a conformation that closely resembles the A-form geometry of RNA−RNA duplexes. It has been reported that LNA monomers alter the sugar pucker of 3′-flanking nucleotides from a preferential S-type pucker in dsDNA duplexes to a mixture of N- and S-type conformations (*45*). In LNA−DNA hybrids, the cognate DNA strands respond to the more A-like geometry of the LNA strand by increasing the population of N-type sugar puckers.

Complete, or partial, compensation between enthalpy (mainly hydrogen bonding energies and van der Waals interactions) and entropy (mostly rearrangements of the molecules, solvent water, and counterions) has been observed for many different biological systems (*47*). The changes in overall binding free energy ($\Delta G°$) can be due to tighter binding (manifested in ΔH) in combination with a larger loss of degrees of freedom (seen in ΔS term). A DNA−DNA association process is entropically unfavorable (reduction in the number of molecules), whereas formation of hydrogen bonds (base pairs) between the two strands and stacking of the bases are enthalpically favored. A modification such as an LNA nucleotide introduced into an oligonucleotide may contribute to either enthalpy or entropy change, or both, in free energy relative to the unmodified duplex. The substituent may form hydrogen bonds and electrostatic and/or hydrophobic interactions when binding to the unmodified complementary DNA or RNA. In terms of thermodynamic parameters, the data in Table 3 suggest that the increased stability of the DNA−LNA duplexes compared to the DNA−DNA duplexes is the net result of the increase in the favorable enthalpy changes of hybridization upon incorporation of first and third modifications and a favorable entropy change upon incorporation of the second modification. The overall effect indicates that in most cases modified duplexes have a larger exothermic contribution than the unmodified duplexes, which suggest that the base stacking interactions in the modified duplexes are more pronounced.

Table 3 also depicts that the effects of LNA modifications on the thermodynamic parameters are differential, suggesting that the effect might be position-dependent or influenced by the nearest neighbors flanking the modification. A position-dependent effect can be ascribed to the fact that presence of first and third modification at the terminus or the near-terminal position produce similar impact on thermodynamic parameters. However, incorporation of a centrally placed second modification, an entirely opposite trend for the $\Delta\Delta H$ and $\Delta\Delta S$ values was observed. The nearest neighbor theory

takes into consideration the placement of an LNA substitution in the vicinity of three different nearest neighbors, i.e., 5′-XG-3′ (first modification), 5′-CXC-3′ (second modification), and 5′-CXG-3′ (third modification), where X is the modified LNA nucleotide. Placing LNA in all three nearest neighbor contexts resulted in an increase in Gibbs free energy. The increment in the Gibbs free energy due to the positioning of LNA in the 5′-CXC-3′ nearest neighbor was mainly due to the contribution from the favorable entropy change, which compensates for the unfavorable enthalpy change. In the other two cases, however, the increase in the Gibbs free energy can be attributed to the large favorable enthalpy change that compensates for the unfavorable entropy change. Similar position-dependent effects for LNA substitutions have been reported in the literature, where a single terminal LNA substitution (5′-XG-3′) failed to generate any considerable influence on hybridization thermodynamics, while an additional internally substituted modification exhibited significant effects (*31*). Furthermore, all the modifications produced small negative $\Delta\Delta H$ and $\Delta\Delta S$ values for duplex formation. This is in contrast to our findings, as we observed a significant change in the thermodynamic profile of the terminally substituted octameric sequence. Additionally, we observed negative $\Delta\Delta H$ and $\Delta\Delta S$ values for the first (5′-XG-3′) and third modification (5′-CXG-3′), while the second modification (5′-CXC-3′) yielded positive values. Our observations are in consensus with the previous studies (*14*, *32*) that report a considerable influence of terminally positioned LNA residues on thermodynamic parameters (*14*), along with an unfavorable enthalpy and a favorable entropy change (positive $\Delta\Delta H$ and $\Delta\Delta S$) associated with 5′-CXC-3′ LNA modification (*32*).

The UV melting studies at several salt concentrations, to examine the thermodynamic uptake of counterions, showed that the increase in the salt concentration resulted in the shift of T_m to higher temperatures. The T_m dependence on salt concentration is shown in Figure 5 for each duplex. From the slopes of these lines ($\delta T_m/\delta \ln[Na^+]$), the thermodynamics of the uptake of counterions (Δn_{Na^+}) for the unmodified and modified duplexes were obtained. It was found that, for duplex formation, incorporation of an extra LNA modification leads to a higher uptake of counterions. This finding can be ascribed to the LNA-induced conformation change of the helix to A-type geometry. Both the linear and three-dimensional charge density of the A-form DNA is known to be high as compared to that of the B-form (*35*, *36*). Relative to the duplex state, the single strands at high temperatures can be considered as true random coils with similar charge density. The higher charge density of the A-type duplexes leads to a higher uptake of counterions upon duplex formation. Further, this increase in the uptake of counterions by the duplex possibly accounts for the unfavorable entropy change associated with the introduction of LNA modification.

It is well established that water molecules bound at specific and/or nonspecific sites along the DNA chain influence the stability of a duplex (*48*−*52*). Determination of effects of hydration on the chemical and physical properties of DNA, thus, depends on evaluation of the quantity of water bound and how the water content changes when DNA undergoes physical or chemical change (*53*−*55*). The knowledge of the hydration changes due to the LNA modification will additionally allow us to identify the origin of enhanced thermal stability of the LNA-modified duplexes. Several physical studies suggest that ∼10 water molecules per nucleotide bind directly to B-DNA as the first layer of hydration (*56*). Extensive hydration of the negative phosphate oxygens and a well-ordered water structure as a spine of hydration in the narrow minor groove of adjacent A-T base pairs (*57*, *58*) or as a ribbon of two side-by-side water molecules in the wider minor groove of adjacent C-G base pairs are documented for B-DNA (*59*, *60*). The major groove of B-DNA is equally well hydrated, but the arrangement of water molecules is irregular. In A-DNA, the negative phosphate oxygens are extensively hydrated as in B-DNA; however, the narrow and deep major groove has a well-ordered network of water molecules arranged as fused pentagons, whereas the shallow and wide minor groove is hydrophobic and not as well hydrated (*61*, *62*). It is, therefore, expected that formation of A-DNA duplexes will be associated with the uptake of less water than the formation of B-DNA duplexes. Our results in Table 4 fully support this notion with a slower uptake of water molecules observed for the A-type modified duplexes. From the CD and NMR studies, it has been observed that the unmodified duplex shows B-type structure, whereas LNA-substituted duplexes adopt an A-type structure (*45*, *46*). Formation of LNA−DNA duplexes generally is, thus, associated with uptake of less water than formation of DNA−DNA duplexes.

CONCLUSION

This study was undertaken to obtain a detailed insight into the hybridization thermodynamics of LNA-modified oligonucleotides. The thermal denaturation experiments with differentially modified duplexes suggested a higher thermal stability for the modified duplexes. Among the adenine (A-LNA) and thymine (T-LNA) substitutions, a slightly higher increment in thermal stability was observed for the thymine-modified duplexes. Complete thermodynamic profile of the differentially modified A- and T-LNA duplexes indicated that the effect of modification on enthalpy−entropy compensation might be positional or affected by the contiguous bases flanking the modification. Further, our UV melting experiments showed that the formation of modified duplexes is associated with higher counterion uptake and a relatively lower uptake of water molecules as compared to those of the unmodified duplexes. This observation can be ascribed to the fact that the incorporation of a LNA modification induces a structural change in the helical geometry to an A-type conformation that possesses a higher charge density but is less hydrated than the B-type conformation of the unmodified duplexes. This structural perturbation associated with LNA incorporation is supported by our CD data that displayed the expected increase in the A-type character of the helix, consistent with a gradual increase in the extent of LNA modification. In the near future, we hope to explore various possible LNA incorporation strategies in different model systems, based on the effect of LNA substitution on thermodynamic parameters. Oligonucleotide behavior is significantly influenced by the presence of LNA modification, which is position-dependent. Investigating hybridization thermodynamics of modified oligonucleotides will aid in predicting their stability, which in turn correlate with their functional efficiency. Furthermore, tracking the effects of

LNA modifications in different sequence contexts will allow us to formulate guidelines for the optimum design of LNA-based oligonucleotides such that maximum functional efficiency could be drawn out of minimum modification.

ACKNOWLEDGMENT

We thank Prof. A. Surolia (MBU, IISc, Bangalore, India) for the use of the VP-DSC calorimeter, which was supported by the Department of Science and Technology, Government of India, under the Intensification of Research in High Priority Areas.

REFERENCES

1. Crooke, S. T. (2004) Progress in antisense technology, *Annu. Rev. Med. 55*, 61−95.
2. Kurreck, J. (2003) Antisense technologies: Improvement through novel chemical modifications, *Eur. J. Biochem. 270*, 1628−1644.
3. Singh, S. K., Nielsen, P., Koshkin, A., and Wengel, J. (1998) LNA (locked nucleic acids): Synthesis and high-affinity nucleic acid recognition, *Chem. Commun.*, 455−456.
4. Wengel, J., Petersen, M., Nielsen, K. E., Jensen, G. A., Håkansson, A. E., Kumar, R., Sorensen, M. D., Rajwanshi, V. K., Bryld, T., and Jacobsen, J. P. (2001) LNA (locked nucleic acid) and the diastereoisomeric α-L-LNA: Conformational tuning and high affinity of DNA/RNA targets, *Nucleosides, Nucleotides Nucleic Acids 20*, 389−396.
5. Koshkin, A. A., Singh, S. K., Nielsen, P., Rajwanshi, V. K., Kumar, R., Meldgaard, M., Olsen, C. E., and Wengel, J. (1998) LNA (Locked Nucleic Acids) synthesis of the Adenine, Cytosine, Guanine, 5-Methylcytosine, Thymine and Uracil bicyclonucleoside monomers, oligomerisation, and unprecedented nucleic acid recognition, *Tetrahedron 54*, 3607−3630.
6. Petersen, M., and Wengel, J. (2003) LNA: A versatile tool for therapeutics and genomics, *Trends Biotechnol. 21*, 74−81.
7. Wahlestedt, C., Salmi, P., Good, L., Kela, J., Johnsson, T., Hokfelt, T., Broberger, C., Porreca, F., Lai, J., Ren, K., Ossipov, M., Koshkin, A., Jakobsen, N., Skouv, J., Oerum, H., Jacobsen, M. H., and Wengel, J. (2000) Potent and nontoxic antisense oligonucleotides containing locked nucleic acids, *Proc. Natl. Acad. Sci. U.S.A. 97*, 5633−5638.
8. Obika, S., Nanbu, D., Hari, Y., Morio, J. A. K., Doi, T., and Imanishi, T. (1998) Stability and structural features of the duplexes containing nucleoside analogues with a fixed N-type conformation, 2′-O,4′-C-methyleneribonucleosides, *Tetrahedron Lett. 39*, 5401−5404.
9. Crinelli, R., Bianchi, M., Gentillini, L., and Magnani, M. (2002) Design and characterization of decoy oligonucleotides containing locked nucleic acids, *Nucleic Acids Res. 30*, 2435−2443.
10. Crinelli, R., Bianchi, M., Gentilini, L., Palma, L., Sørensen, M. D., Bryld, T., Babu, R. B., Arar, K., Wengel, J., and Magnani, M. (2004) Transcription factor decoy oligonucleotides modified with locked nucleic acids: An in vitro study to reconcile biostability with binding affinity, *Nucleic Acids Res. 32*, 1874−1885.
11. Chernolovskaya, E. L., Koshkin, A. A., and Vlassov, V. V. (2001) Interaction LNA oligonucleotides with mdr-1 promoter, *Nucleosides, Nucleotides Nucleic Acids 20*, 847−850.
12. Schmidt, K. S., Borkowski, S., Kurreck, J., Stephens, A. W., Bald, R., Hecht, M., Friebe, M., Dinkelborg, L., and Erdmann, V. A. (2004) Application of locked nucleic acids to improve aptamer in vivo stability and targeting function, *Nucleic Acids Res. 32*, 5757−5765.
13. Braasch, D. A., and Corey, D. R. (2001) Locked nucleic acids (LNA): Fine-tuning the recognition of DNA and RNA, *Chem. Biol. 8*, 1−7.
14. Kurreck, J., Wysko, E., Gillen, C., and Erdmann, V. A. (2002) Design of antisense oligonucleotides stabilized by locked nucleic acid, *Nucleic Acids Res. 30*, 1911−1918.
15. Hansen, J. B., Westergaard, M., Thrue, C. A., Giwercman, B., and Oerum, H. (2003) Antisense knockdown of PKC-α using LNA-oligos, *Nucleosides, Nucleotides Nucleic Acids 22*, 1607−1609.
16. Jepsen, J. S., Pfunheller, H. M., and Lykkesfeldt, A. E. (2004) Downregulation of p21 and estrogen receptor α in MCF-7 cells by antisense oligonucleotides containing locked nucleic acid (LNA), *Oligonucleotides 14*, 147−156.
17. Fluiter, K., Ten Asbroek, A. L., De Wissel, M. B., Jacobs, M. E., Wissenbach, M., Olsson, H., Olsson, O., Oerum, H., and Baas, F. (2002) In vivo tumor growth inhibition and biodistribution studies of locked nucleic acid (LNA) antisense oligonucleotides, *Nucleic Acids Res. 31*, 953−962.
18. Obika, S., Hemamayi, R., Masuda, T., Sugimoto, T., Nakagawa, S., Mayumi, T., and Imanishi, T. (2001) Inhibition of ICAM gene expression by 2′,4′-BNA oligonucleotides, *Nucleic Acids Res. (Suppl.) 1*, 145−146.
19. Nulf, C. J., and Corey, D. (2004) Intracellular inhibition of hepatitis C virus (HCV) internal ribosomal entry site (IRES)-dependent translation by peptide nucleic acids (PNAs) and locked nucleic acids (LNAs), *Nucleic Acids Res. 32*, 3792−3798.
20. Grunweller, A., Wyszko, E., Bieber, B., Jahnel, R., Erdmann, V. A., and Kurreck, J. (2003) Comparison of different antisense strategies in mammalian cells using locked nucleic acids, 2′-O-methyl RNA, phosphorothioates and small interfering RNA, *Nucleic Acids Res. 31*, 3185−3193.
21. Fahmy, R. G., and Khachigian, L. M. (2004) Locked nucleic acid modified DNA enzymes targeting early growth response-1 inhibit human vascular smooth muscle cell growth, *Nucleic Acids Res. 32*, 2281−2285.
22. Childs, J. L., Disney, M. D., and Turner, D. H. (2002) Oligonucleotide directed misfolding of RNA inhibits *Candida albicans* group I splicing, *Proc. Natl. Acad. Sci. U.S.A. 99*, 11091−11096.
23. Elayadi, A. N., Braasch, D. A., and Corey, D. R. (2002) Implications of high affinity hybridization by locked nucleic acids for inhibition of human telomerase, *Biochemistry 41*, 9973−9981.
24. Arzumanov, A., Walsh, A. P., Rajewanshi, V. K., Kumar, R., Wengel, J., and Gait, M. J. (2001) Oligonucleotide analogue interference with the HIV-1 Tat protein-TAR RNA interaction, *Nucleosides, Nucleotides Nucleic Acids 20*, 471−480.
25. Lattora, D., Hopkins, D., Campbell, K., and Hurley, J. M. (2003) Multiplex allele specific PCR with optimized locked nucleic acid primers, *BioTechniques 34* (6), 1150−1152.
26. Jacobsen, N., Bentzen, J., Meldgaard, M., Jakobsen, M. H., Fenger, M., Kauppinen, S., and Skouv, J. (2002) LNA-enhanced detection of single nucleotide polymorphisms in the apolipoprotein E, *Nucleic Acids Res. 30*, e100.
27. Jacobsen, N., Fenger, M., Bentzen, J., Rasmussen, S., Jakobsen, M., Fenstholt, J., and Skouv, J. (2002) Genotyping of the apolipoprotein B R3500Q mutation using immobilized locked nucleic acid capture probes, *Clin. Chem. 48*, 657−660.
28. Orum, H., Jakobsen, M. H., Koch, M. H., Vuust, J., and Borre, M. B. (1999) Detection of the Factor V Leiden Mutation by Direct Allele-specific Hybridization of PCR Amplicons to Photoimmobilized Locked Nucleic Acids, *Clin. Chem. 9*, 1898−1905.
29. Simeonov, A., and Nikiforav, T. T. (2002) Single nucleotide polymorphism genotyping using short, fluorescently labeled locked nucleic acid (LNA) probes and fluorescence polarization detection, *Nucleic Acids Res. 30*, e31.
30. Koshkin, A. A., Nielsen, P., Meldgaard, M., Rajwanshi, V. K., Singh, S. K., and Wengel, J. (1998) LNA (Locked Nucleic Acid): An RNA mimic forming exceedingly stable LNA:LNA duplexes, *J. Am. Chem. Soc. 120*, 13252−13253.
31. Christensen, U., Jacobsen, N., Rajwanshi, V. K., Wengel, J., and Koch, T. (2001) Stopped-flow kinetics of locked nucleic acid (LNA)-oligonucleotide duplex formation: Studies of LNA-DNA and DNA-DNA interactions, *Biochem. J. 354*, 481−484.
32. McTigue, P. M., Peterson, R. J., and Kahn, J. D. (2004) Sequence-dependent thermodynamic parameters for locked nucleic acid (LNA)-DNA duplex formation, *Biochemistry 43*, 5388−5405.
33. Cantor, C. R., Warshaw, M. M., and Shapiro, H. (1970) Oligonucleotide interactions. III. Circular dichroism studies of the conformation of deoxyoligonucleotides, *Biopolymers 9*, 1059−1077.
34. Marky, L. A., Blumenfeld, K. S., Kozlowski, S., and Breslauer, K. J. (1983) Salt-dependent conformational transitions in the self-complementary deoxydodecanucleotide d(CGCAATTCGCG): Evidence for hairpin formation, *Biopolymers 22*, 1247−1257.
35. Marky, L. A., and Breslauer, K. J. (1987) Calculating thermodynamic data for transitions of any molecularity from equilibrium melting curves, *Biopolymers 26*, 1601−1620.
36. Rentzeperis, D., Kharakoz, D. P., and Marky, L. A. (1991) Coupling of sequential transitions in a DNA double hairpin: Energetics, ion binding and hydration, *Biochemistry 30*, 6276−6283.

37. Spink, C. H., and Chaires, J. B. (1999) Effects of hydration, ion release and excluded volume on the melting of triplex and duplex DNA, *Biochemistry 38*, 496−508.
38. Soto, A. M., Kankia, B. I., Dande, P., Gold, B., and Marky, L. A. (2001) Incorporation of a cationic aminopropyl chain in DNA hairpins: Thermodynamics and hydration, *Nucleic Acids Res. 29*, 3638−3645.
39. Soto, A. M., Kankia, B. I., Dande, P., Gold, B., and Marky, L. A. (2002) Thermodynamic and hydration effects for the incorporation of a cationic 3-aminopropyl chain into DNA, *Nucleic Acids Res*. *30*, 3171−3180.
40. Johnson, W. C. (1994) CD of nucleic acids, in *Circular Dichroism: Principles and Applications* (Nakanishi, K., Berova, N., and Woody, R. W., Eds.) pp 523−540, VCH, New York.
41. Manning, G. S. (2002) Electrostatic free energy of the DNA double helix in counterion condensation theory, *Biophys. Chem. 101*−*102*, 461−473.
42. Jayaram, B., Sprous, D., Young, M. A., and Beveridge, D. L. (1998) Free energy analysis of the conformational preferences of A and B forms of DNA in solution, *J. Am. Chem. Soc*. *120*, 10629−10633.
43. Zieba, K., Chu, T. M., Kupke, D. W., and Marky, L. A. (1991) Differential hydration of dA·dT base pairing and dA and dT bulges in deoxyoligonucleotides, *Biochemistry 30*, 8018−8026.
44. Marky, L. A., Rentzeperis, D., Luneva, N. P., Cosman, M., Geacintov, N. E., and Kupke, D. W. (1996) Differential hydration thermodynamics of stereoisomeric DNA-benzo[*a*]pyrene adducts derived from diol epoxide enantiomers with different tumorigenic potentials, *J. Am. Chem. Soc*. *118*, 3804−3810.
45. Bondensgaard, K., Petersen, M., Singh, S. K., Rajwanshi, V. K., Kumar, R., Wengel, J., and Jacobsen, J. P. (2000) Structural studies of LNA:RNA duplexes by NMR: Conformations and implications for RNase H activity, *Chem.*−*Eur. J. 6*, 2687−2685.
46. Petersen, M., Bondensgaard, K., Wengel, J., and Jacobsen, J. P. (2002) Locked nucleic acid (LNA) recognition of RNA: NMR solution structures of LNA:RNA hybrids, *J. Am. Chem. Soc*. *124*, 5974−5982.
47. Marky, L. A., and Kupke, D. W. (2000) Enthalpy−entropy compensations in nucleic acids: Contribution of electrostriction and structural hydration, *Methods Enzymol*. *323*, 419−441.
48. Texter, J. (1979) Nucleic acid−water interactions, *Prog. Biophys. Mol. Biol*. *33*, 83−97.
49. Berman, H. M. (1991) Hydration of DNA, *Curr. Opin. Struct. Biol*. *1*, 423−427.
50. Berman, H. M. (1994) Hydration of DNA, take 2, *Curr. Opin. Struct. Biol*. *4*, 345−350.
51. Kochoyan, M., and Leroy, J. L. (1995) Hydration and solution structure of nucleic acids, *Curr. Opin. Struct. Biol*. *5*, 329−333.
52. Westhoff, E. (1988) Water: An integral part of nucleic acid structure, *Annu. Rev. Biophys. Biophys. Chem*. *17*, 125−144.
53. Kankia, B. I., and Marky, L. A. (1999) DNA, RNA and DNA/RNA oligomer duplexes: A comparative study of their stability, heat, hydration and Mg^{2+} binding properties, *J. Phys. Chem. B 103*, 8759−8767.
54. Kankia, B. I., and Marky, L. A. (2001) Folding of the thrombin aptamer into a G-quadruplex with Sr^{2+}: Stability, heat and hydration, *J. Am. Chem. Soc. 123*, 10799−10804.
55. Kankia, B. I., Kupke, D. W., and Marky, L. A. (2001) The incorporation of a platinated cross-link into duplex DNA yields an uptake of structural water, *J. Phys. Chem. B 105*, 11402−11405.
56. Feig, M., and Pettitt, B. M (1999) A molecular simulation picture of DNA hydration around A- and B-DNA, *Biopolymers 48*, 199−209.
57. Drew, H. R., Wing, R. M., Takano, T., Broka, C., Tanaka, S., Itakura, K., and Dickerson, R. E. (1981) Structure of a B-DNA Dodecamer: Conformation and Dynamics, *Proc. Natl. Acad. Sci. U.S.A. 78*, 2179−2183.
58. Drew, H. R., and Dickerson, R. E. (1981) Structure of a B-DNA dodecamer: III. Geometry of hydration, *J. Mol. Biol. 151*, 535−556.
59. Prive, G. G., Yanagi, K., and Dickerson, R. E. (1991) Structure of the B-DNA decamer C-C-A-A-C-G-T-T-G-G and comparison with isomorphous decamers C-C-A-A-G-A-T-T-G-G and C-C-A-G-G-C-C-T-G-G, *J. Mol. Biol. 217*, 177−199.
60. Tereshko, V., Minasov, G., and Egli, M. (1999) A "Hydrat-Ion" spine in a B-DNA minor groove, *J. Am. Chem. Soc. 121*, 3590−3595.
61. Conner, B. N., Yoon, C., Dickerson, J. L., and Dickerson, R. E. (1984) Helix geometry and hydration in an A-DNA tetramer: ^{1}C-C-G-G, *J. Mol. Biol. 174*, 663−695.
62. Kennard, O., Cruse, W. B. T., Nachman, J., Prange, T., Shakked, Z., and Rabinovich, D. (1986) Ordered water structure in an A-DNA octamer at 1.7 Å resolution, *Biomol. Struct. Dyn. J. 3*, 623−647.

BI060307W